Journal of Environmental Chemical Engineering 10 (2022) 107378

Contents lists available at ScienceDirect

Journal of Environmental Chemical Engineering

journal homepage: www.elsevier.com/locate/jece

Mild sulphuric acid pre-treatment for metals removal from biosolids and the fate of metals in the treated biosolids derived biochar

Ibrahim Gbolahan Hakeem [a,b], Pobitra Halder [a,b], Mojtaba Hedayati Marzbali [a], Savankumar Patel [a,b], Nimesha Rathnayake [a,b], Aravind Surapaneni [b,c], Graeme Short [c], Jorge Paz-Ferreiro [a], Kalpit Shah [a,b,*]

[a] Chemical and Environmental Engineering, School of Engineering, RMIT University, Melbourne, VIC 3000, Australia
[b] ARC Training Centre for the Transformation of Australia's Biosolids Resources, RMIT University, Bundoora, VIC 3083, Australia
[c] South East Water Corporation, Frankston, VIC 3199, Australia

ARTICLE INFO

Editor: V. Victor

Keywords:
Acid leaching
Demineralization
Heavy metals
Pyrolysis
Biochar
Alkali and alkaline earth metals

ABSTRACT

Biosolids are contaminated with heavy metals (HMs) and alkali and alkaline earth metals (AAEMs). These metals limit the suitability of biosolids for land application as well as their pyrolytic conversion to high-quality products. In this work, a mild sulphuric acid pre-treatment of biosolids was carried out at different stirring speeds (300–900 rpm), temperatures (25–100 °C), extraction time (0–180 min), and acid concentration (1–5% v/v) to reduce the metals load in biosolids and their biochar derived from pyrolysis. The metal leaching process was very rapid and reached equilibrium in less than 30 min. The optimum conditions removed about 75–95% HMs and 80–95% AAEMs except Ca due to the formation of $CaSO_4$ hydrates. Temperature was the driving parameter for Cd and Ni extraction, whereas temperature and acid concentration played the leading roles in Cu extraction. The shrinking core product layer diffusion and surface chemical reaction models described the extraction kinetics of Ni, Cu and Cd. A leaching activation energy of 10.02 kJ/mol and 7.37 kJ/mol was estimated for Ni and Cd, respectively. FTIR, SEM and XRD characterisation of the treated biosolids jointly indicated that the leaching mechanism was dominated by acid dissolution of metal-containing components followed by ion exchange of metal species with protons from H_2SO_4. Treatment at 25 °C and 3% H_2SO_4 lowered the biosolids ash content by 50% and preserved the physicochemical attributes, which enhanced the pyrolysis upcycling of the treated biosolids. Pre-treatment influenced the migration characteristics of the metals during pyrolysis and the produced biochar had several folds lower HMs and AAEMs contents than the raw biosolids-derived biochar.

1. Introduction

The sustainable management of the increasing biosolids remains a big hurdle for the wastewater industry and research community. Traditional biosolids management spans across landfilling, incineration, composting, stockpiling and recently thermochemical processing for resource recovery [1,2]. In many countries, land application in agricultural soils is the predominant management route [3]. For instance, in Australia, about 70% of biosolids are beneficiated to agricultural land because of their nutritional organic and inorganic (mainly N, P, K) constituents [4]. However, the increase in emerging contaminants such as per- and poly-fluoroalkyl substances, pesticides, microplastics, and heavy metals (HMs) in biosolids are limiting their direct land application. Controlled HMs in biosolids include As, Cr, Cd, Cu, Hg, Pb, Ni, Se, and Zn, and their concentrations can be higher than the safe limit prescribed by many environmental legislations [1,3,5,6]. As a result, in Victoria, Australia, only the least contaminant (C-1) and highest treatment (T-1) grades biosolids have unrestricted applications in agricultural land [5].

Thermochemical treatment can be an attractive management option for biosolids that cannot be used conventionally in agricultural soils due to concerns with environmental pollution. Pyrolysis is a widely studied method for converting biosolids to biochar (carbon and nutrient-rich solid), bio-oil (condensable volatiles liquid) and pyrolysis gas (non-condensable gases) [7–10]. Pyrolysis can degrade the persistent organic contaminants and pathogens in biosolids and reduce the waste volume significantly [11,12]. However, pyrolysis concentrates inorganic constituents such as HMs, alkali and alkaline earth metals (AAEMs) and

* Corresponding author at: Chemical and Environmental Engineering, School of Engineering, RMIT University, Melbourne, VIC 3000, Australia.
E-mail address: kalpit.shah@rmit.edu.au (K. Shah).

https://doi.org/10.1016/j.jece.2022.107378
Received 13 November 2021; Received in revised form 30 January 2022; Accepted 10 February 2022
Available online 12 February 2022

silicates in the resulting biochar. This is due to the degradation of organic matter during pyrolysis and the thermal stability of the metals [13]. The elevated HMs contents in the biochar could hinder their direct land application similar to the parent biosolids. Also, excessive levels of AAEMs in biochar can weaken the oxidation resistance of the biochar carbon, lower the ash fusion temperature, and induce slagging and fouling during combustion [14,15]. While the metals are largely retained in the biochar after pyrolysis, they have many deleterious effects on the pyrolysis process and products formation [16–18]. Moreover, the possible migration of HMs from biosolids to oil and gas fractions during pyrolysis has raised environmental concerns [19,20]. Therefore, the removal of HMs and AAEMs from biosolids could be beneficial for selective product formation during pyrolysis as well as for the enhancement of biosolids and their char quality.

Several methods are demonstrated in literature for metals removal from biosolids [21,22]. The use of mineral and organic acids [23,24], chelating agents [25], ionic liquids [26], surfactants [27], ferric salts [28,29], and bioleaching [30] have been reported. Acidification can be the most promising technique for concurrent biosolids demineralisation, hydrolysis, and HMs solubilisation while preserving the organic residue (high-grade pre-treated biosolids with a low concentration of HMs and AAEMs) for pyrolysis upcycling or land application [21,31,32]. Previous studies on biosolids acid pre-treatment mainly focused on HMs extraction from contaminated/industrial biosolids with no pyrolysis investigation of the pre-treated biosolids [33–36]. As such, very harsh pre-treatment conditions are used to remove HMs from biosolids before disposal or land application. The harsh conditions usually result in the breakdown of the biosolids' valuable organic matter during the pre-treatment. Owing to its low cost, industrial maturity, and effectiveness, sulphuric acid (H_2SO_4) is a popular leaching solvent. Considerable variation exists among studies on the removal efficiency of HMs from municipal biosolids using H_2SO_4 due to several opposing factors such as solids concentration, temperature, acid concentration (or pH), stirring speed and extraction time [24,32,37,38]. For instance, Stylianou et al. [32] reported over 70% removal of Ni, Cu, Cr and Zn from municipal biosolids at an optimum condition of 20% (v/v) H_2SO_4 and 80 °C for 30 min. In contrast, removal of 82% Cr, 25% Cu, 80% Ni, 50% Pb and 70% Zn was achieved at 20% (v/v) H_2SO_4 and room temperature for 60 min in another work [24]. The extraction kinetics of HMs leaching from biosolids using H_2SO_4, which is necessary to develop scale-up process designs for biosolids treatment and to understand the feasibility of integrating within the existing infrastructure of water treatment plants, are scarce in the literature [33]. Studies published on the kinetics of HMs extraction using acids are only applied to hazardous wastes and metals-ores [39–42].

Limited studies on integrated acid pre-treatment and pyrolysis were centred on understanding the role of inherent biosolids metals on their thermal decomposition behaviour and kinetics [43–45]. The analytical pyrolysis of acid demineralised biosolids or demineralised biosolids spiked with specific metals/minerals demonstrated the catalytic role of metals in fostering or inhibiting gaseous pollutants release, thermal degradation stability of organic macromolecules, and pyrolysis activation energy. Removing ash-forming elements from biosolids by H_2SO_4 treatment was reported to improve devolatilisation and denitrogenation reactions during the catalytic pyrolysis of the treated biosolids to co-produce hydrocarbons and ammonia [31]. However, the effect of pre-treatment and subsequent pyrolysis on the metal contents in the biosolids derived biochar was not reported. Also, previous studies [31, 46] lack detailed physicochemical characterisation of acid pre-treated biosolids, which is crucial in understanding the effects of acid treatment under a wide range of conditions and for assessing the suitability of the treated biosolids for appropriate applications.

Reducing biosolids HMs contaminants load through mild H_2SO_4 treatment can upgrade the quality of low-grade biosolids that are ordinarily unfit for agricultural application suitable for unrestricted land use. Also, the pyrolytic conversion of upgraded biosolids to high-quality biochar and bio-oil can enhance value recovery from biosolids. No single study has reported a comprehensive insight into the integrated chemical and thermal treatment of biosolids. Therefore, this study aims to employ mild H_2SO_4 (1–5% v/v) pre-treatment to obtain high-quality biosolids and biochar with respect to HMs concentration. The whole spectrum of biosolids H_2SO_4 treatment for metals removal, involving process optimisation, leaching kinetics and mechanistic insights, and physicochemical characterisation, were studied. The effect of pyrolysis on the subsequent concentration of the metals in the derived biochar was investigated. Specific objectives were to (i) investigate the role of pre-treatment process parameters (temperature, acid concentration and stirring rates) on the extraction behaviour of AAEMs and controlled HMs from Australian biosolids, (ii) estimate the leaching kinetic parameters using the shrinking core models, (iii) study the effects of pre-treatment process parameters on biosolids physicochemical, thermal and structural properties, and (iv) examine the influence of pre-treatment and pyrolysis on the fate of metals in the biosolids derived biochar.

2. Materials and Methods

2.1. Sample collection and preparation

The biosolids used in this study was obtained from Mount Martha wastewater recycling plant, South East water corporation, Melbourne, Australia. The plant uses anaerobic digestion and lagoon treatment for sludge concentration. The concentrated sludge is dosed with polymer additives to coalesce the flocs, followed by mechanical dewatering using a belt-press filter and drying using a solar dryer. The biosolids employed in this study are the final solids from the dryer. Before further use, the biosolids sample was oven-dried at 105 °C and sieved to 100–400 μm particle sizes. The ultimate and proximate analyses, as well as their metals compositions, are presented in Table SI1. The raw biosolids contain higher concentrations of Cd, Cu, and Zn than those of C-1 grade biosolids (the least contaminant grade, according to Victoria (Australia) EPA biosolids guidelines [5]. Therefore, the extraction of Cd, Cu, Ni, and Zn (HMs) alongside Na, K, Mg, and Ca (AAEMs) were investigated in this study. The chemicals used were of analytical grades and included sulphuric acid (s.gr 1.64, 98% Assay, RCI Labscan Ltd), 70% nitric acid (Merck Pty Ltd), and 30% hydrogen peroxide (Rowe Scientific Pty Ltd). Deionised 18.2 MΩ.cm Milli-Q water (Milli-pore Corporation) was used throughout this work.

2.2. Pre-treatment procedure

The batch pre-treatment experiment was conducted in 20 ml glass vials immersed in a temperature-controlled oil bath on a magnetic stirrer hot plate (Super-Nuova$^+$ Thermo Scientific). The vials were capped tightly to avoid evaporation losses and keep the solid mass ratio constant. Dried biosolids and H_2SO_4 (pH <2) was used in a solid to liquid ratio of 1:10 (g/ml). The influence of temperature (25–100 °C), acid concentration (1–5% v/v), stirring speed (300–900 rpm), and time (0–180 min) was investigated on AAEMs and HMs extraction. For the investigation of single parameter effect on metal extraction rates, other parameters values were kept constant at 63 °C, 3% acid, and 600 rpm. The process parameters were optimised using the Box-Behnken response surface methodology design. The range and levels of the factors (acid concentration, temperature, and time) are shown in Table SI2.

A typical pre-treatment experiment involved heating 10 ml of H_2SO_4 with a known concentration to the desired temperature (±3 °C). Then, 1 g of dried biosolids were added to the pre-heated acid solution, a magnetic stirrer bar was inserted into the vial, and the vial was tightly capped. The reaction lasted for 180 ± 2 min under continuous stirring at the desired rpm. The slurry was then vacuum filtered to separate into an aqueous stream (leachate) and solid residue. Aliquot of the leachate was filtered using NY 0.45 μm syringe filter, diluted and quantified for metals using ICP-MS. The dissolved metal concentration in the leachate

(mg/kg dry biosolids) was calculated by Eq. (1), and the metals extraction fraction was calculated by Eq. (2). The residue was washed with deionised water until the filtrate approached neutral pH. The treated biosolids were dried and stored for further analysis. Each pre-treatment experiment was carried out at least in triplicates, and the average results are presented in the manuscript. Experimental and measurement errors are reported as the standard deviation of the data. Pre-treated samples are denoted as Sample number (pre-treatment conditions) – for instance, S1(25−1−1) denoted Sample 1 obtained at 25 °C and 1% acid for 1 hr.

$$C_{M,leachate}\ \left(\frac{mg}{kg}\right) = \frac{C_{M,leachate}\ \left(\frac{mg}{L}\right)\ X\ V\ (L)}{W\ (kg)} \tag{1}$$

$$Extraction\ \ fraction\ _M = \frac{C_{M,leachate}\ \left(\frac{mg}{kg}\right)}{C_{M,biosolids}\ \left(\frac{mg}{kg}\right)} \tag{2}$$

Where: M denote metal component and $C_{M,leachate}$ is the concentration of metal dissolved in the leachate, $C_{M,biosolids}$ is the metal concentration in the biosolids feed, V is the total leachate volume, W is the dry mass of biosolids.

2.3. Leaching kinetics

Metal extraction is usually described as a solid-liquid phase heterogeneous reaction and can be regarded as a leaching process. The shrinking core kinetic model is a popular correlation used to estimate leaching kinetic parameters [39,47,48]. The model offers a good approximation of real particles behaviour than other reaction models in a wide variety of situations [49]. Eqs. (3)–(5) can be used to describe the shrinking core models for each of the leaching phenomenon [40,50].

i) If the reaction rate is diffusion-controlled through the liquid film (external diffusion effects), the rate expression is:

$$\alpha_i = k_{d,l}t \tag{3}$$

ii) If the reaction rate is controlled by diffusion through the product/ash layer (internal diffusion effects), the rate expression becomes

$$1 - 2\Big/3\alpha_i - (1-\alpha_i)^{2/3} = k_{d,s}t \tag{4}$$

iii) If the reaction rate is controlled by surface chemical reaction (phase boundary reaction), the rate expression becomes

$$1 - (1-\alpha_i)^{1/3} = k_{r,s}t \tag{5}$$

iv) For each of the cases, the temperature dependence of the apparent rate constant can be correlated by the Arrhenius expression

$$k_x = Ae^{\left(-\frac{E_a}{RT}\right)} \tag{6}$$

Where: α_i is the extraction fraction of metal i, $k_{d,l}$ is the liquid diffusion rate constant, $k_{d,s}$ is the product layer diffusion rate constant, $k_{r,s}$ is the chemical reaction rate constant, t is the extraction time (min), k_x is the overall apparent rate constant, A is the pre-exponential factor, R is the universal gas constant (8.314 kJ/mol K), E_a is the activation energy (kJ/mol), and T is the absolute temperature (K). Experimental data (metals extraction fraction and time) were fitted to Eqs. (3)–(5) to determine the leaching mechanisms and kinetic parameters. The coefficient of correlation (R^2) value and near-zero intercept of the linear relationship was used to assess the appropriate fit of the experimental data to the kinetic model equations. Finally, the leaching E_a was estimated by fitting appropriate rate constants to the Arrhenius correlation (Eq. 6).

2.4. Physicochemical characterisation of treated biosolids

2.4.1. Ultimate and proximate analyses

Proximate analysis of treated biosolids was performed using a Simultaneous Thermal Analyser (STA 6000 Perkin Elmer), and ultimate analysis was performed in a CHNS 2400 Series II Perkin Elmer. The oxygen content was obtained by difference on a dry ash-free basis. Both analyses were performed in triplicates, and the results were the average of three runs with errors expressed as the standard deviation of the measurements.

2.4.2. Minerals and metals analyses

The minerals (metal oxides) compositions of treated and raw samples were determined using an X-ray Fluorescence (XRF, AXS S4 Pioneer Bruker) instrument. The major mineral species in the raw and treated samples were identified through an X-ray Diffractometry (XRD, AXS D4 Pioneer Bruker) analysis. Trace metals were determined using Inductive Coupled Plasma-Mass Spectrometry (ICP-MS 7700 Series, Agilent Technologies) instrument following acid digestion of biosolids samples according to method 3050B [51]. Briefly, 0.25 g of dried biosolids sample was weighed into thermal glass vessels. Then 5 ml of 70% HNO_3 was added to the biosolids, and the mixture was refluxed at 95 °C for 2 hr in a digester block (DK 42/26, VELP Scientifica). The procedure was repeated until no brown fumes were given off, indicating complete oxidation in HNO_3. After cooling, the solution was concentrated to the required volume by drying at 65 °C. Then 2 ml of 30% H_2O_2 was added to the solution, followed by heating at 95 °C for 20 min. This step was repeated several times with the addition of 1 ml H_2O_2 until no effervescence was observed. The digested solution was centrifuged, filtered and diluted appropriately for metals quantification in ICP-MS.

2.4.3. Functional groups distribution

The functional groups present in raw and treated biosolids as well as their biochar were identified using a Fourier Transformed Infrared Spectroscopy (FTIR, Spectrum 100, Perkin Elmer). The FTIR spectra were captured in absorbance mode over a scanning wavelength of 4000–400 cm^{-1} at 32 scanning times and 4 cm^{-1} resolutions.

2.4.4. Structural properties

A scanning electron microscope ((SEM), FEI Quanta 200, USA) was used to analyse the surface morphologies of raw and treated biosolids samples. Before SEM imaging, all samples are securely placed on an aluminium stub with carbon tape and coated with iridium using Leica EM ACE 600 sputter coating instrument. The SEM instrument was operated at 30 kV voltage, and SEM images were captured at the same spot size (5.0) and magnification (×3000) to compare the surface morphology. Brunauer–Emmett–Teller (BET) surface area of raw and acid-treated biosolids samples was measured using the Micromeritics TriStar II instrument (nitrogen gas sorption at 77 K). Before the analysis, the samples were degassed under vacuum for at least 20 hr at 180 °C in a Micrometrics VacPrep 061 system.

2.4.5. Thermogravimetric analysis

The thermal degradation behaviour of raw and treated biosolids was assessed using TGA 8000 (Perkin Elmer, USA). Five milligrams of each sample was heated from 35 to 800 °C at a heating rate of 20 °C/min under a pure nitrogen atmosphere flowing at 20 ml/min. TG and DTG profiles were obtained as plots of %mass loss and derivative mass loss versus temperature, respectively.

2.5. Fate of metals in biosolids biochar

Biosolids treated at 63 °C and 3% H_2SO_4 for 2 hr (conditions selected from the optimisation results) was used to produce biochar at 500 °C in a muffle furnace for 3 hr residence time. Similarly, raw biosolids biochar was also produced at the same conditions to compare the HMs contents in the two char products. Biochar from treated biosolids (TB) and raw biosolids (RB) was denoted as TBB and RBB, respectively. The metal *i* retention factor (MRF_i), calculated by Eq. (7), was used to demonstrate the effect of pyrolysis on metal concentration in the biochar [52]. The recovery of metal *i* (R_i) in the char products after pyrolysis was calculated by Eq. (8) [19].

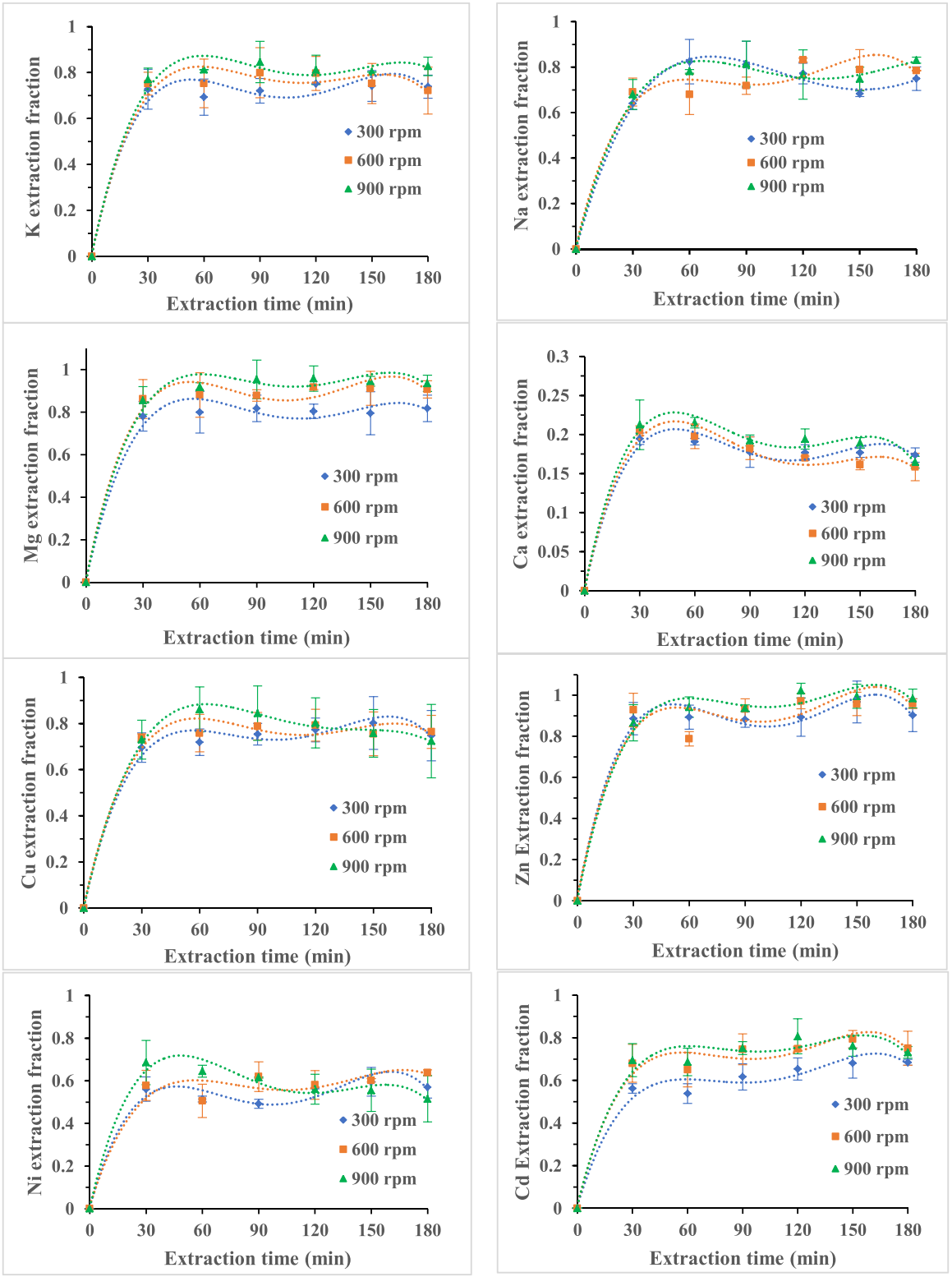

Fig. 1. Effects of stirring speeds on the extraction rate of AAEMs and controlled HMs at 63 °C, 3% H_2SO_4, and 1:10 (g/ml S/L).

$$MRF_i = \frac{Amount\ \ of\ \ metal\ \ i\ \ \left(\frac{mg}{kg}\right)\ \ in\ \ biochar}{Amount\ \ of\ \ metal\ \ i\ \ \left(\frac{mg}{kg}\right)\ \ in\ \ biosolids\ \ feed} \quad (7)$$

$$R_i(\%) = \ \ MRF_i\ \ X\ \ biochar\ \ yield\ \ (wt\%) \quad (8)$$

3. Results and Discussion

3.1. Effects of pre-treatment process parameters on metals extraction

3.1.1. Effects of stirring speeds

The extraction profile of AAEMs (Na, K, Mg, Ca) and HMs (Cu, Zn, Ni, Cd) at three stirring speeds (300, 600 and 900 rpm), 63 °C and 3%

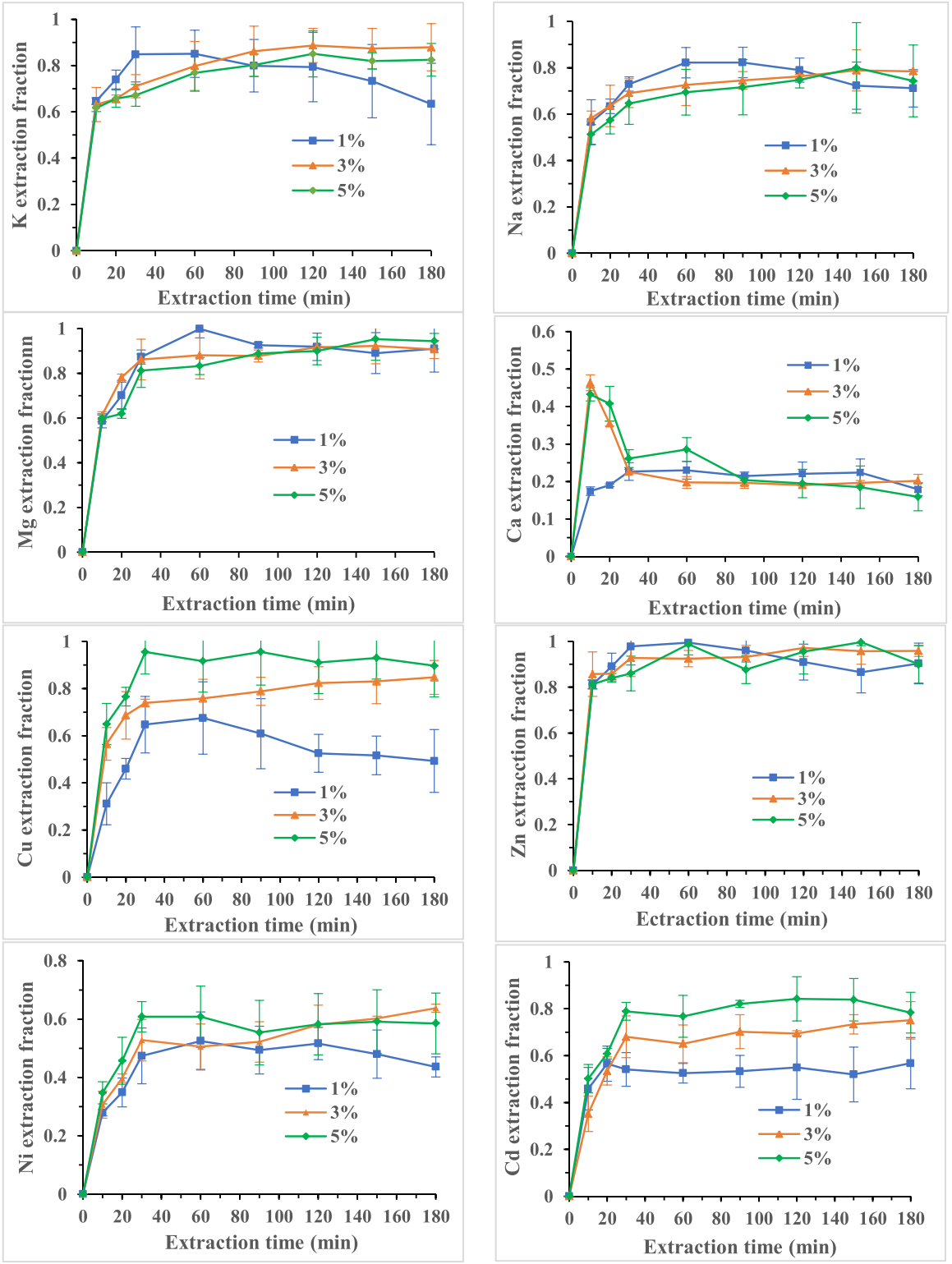

Fig. 2. Effects of acid concentrations on the extraction rate of AAEMs and controlled HMs at 63 °C, 600 rpm and 1:10 (g/ml S/L).

H_2SO_4 is shown in Fig. 1. The profile illustrates the effect of external mass transfer (film diffusion barrier) on the metals extraction rates. The extraction behaviour of all the metals was quite similar, as the extraction rate rapidly increased up to the first 30 min and then became relatively stable. For most of the metals, increasing stirring speed from 300–900 rpm was inconsequential on the extraction rates. Whereas, the extraction rate of few of the metals (such as Mg and Cd) increased when the stirring speed increased from 300 to 600 rpm; however, negligible improvements were observed from 600 to 900 rpm. The very close or overlapping extraction profile at 600–900 rpm indicated that the extraction kinetics of each metal element was neither limited nor controlled by external film diffusion. Hence, the apparent reaction rate can be dominated by internal diffusion or surface chemical reaction phenomena. Therefore, 600 rpm was selected as the optimum working speed for subsequent experiments. It can be seen from Fig. 1 that the pre-treatment at 600 rpm extracted about 70–95% of all metals excluding Ca in the first 30 min suggesting the dominance of an extremely fast ion-exchange reaction between the metal cations and protons from H_2SO_4. Remarkable scatter exists among studies on the optimum stirring speeds and their effects on metals extraction using H_2SO_4 [41,49,53]. Differences in feed materials, chemical speciation of the metals within the feed matrix, and process conditions contribute to the varied influence of stirring speed on metals extraction. The influence of agitation speed may not be negligible at very low rpm and in the early stage of the process where the external mass transfer barrier would be prominent [54]. However, the influence will depend on feed parameters, particularly particle size, since external mass diffusion theory is a function of particle size ($k \sim 1/d_p$) with diffusion coefficient (k) increasing with decreasing particle diameter (d_p) [41].

3.1.2. Effects of acid concentration

The effect of acid concentration (i.e., 1–5% v/v) at 63 °C and 600 rpm on the extraction profiles of the metal elements is shown in Fig. 2. The regression analysis and one-way ANOVA of the parameter can be found in Table SI3. The effect of acid concentration was not significant ($p > 0.05$) on the extraction rate of most metals. For Na, K, Mg and Zn, the lowest acid concentration (1%) extracted maximum metals corresponding to 82%, 85%, 99% and 99% in the first 60 min. However, higher acid concentration (3–5%) enhanced the extraction stability of the metals, as the extraction rate for the metals dropped after 60 min using 1% acid. H_2SO_4 was reported to have good selectivity to Zn, reaching to100% extraction in previous literature [55,56]. Zn and Cu are the two limiting HMs in the biosolids; however, the lower affinity of Zn towards the organic ligands compared to Cu could also explain its stronger solubilisation at all acid concentrations [28]. Alkali metals (Na and K), unlike the alkaline earth metals (Mg and Ca), are very reactive and highly water-soluble [57]. Ca extraction was significantly influenced ($p < 0.05$) by acid concentration in the first 10 min. The two-fold extraction (45%) of Ca in the first 10 min probably occurred before the formation of $CaSO_4$, and the extraction decreased monotonically with time as more $CaSO_4$ was formed until no further extraction was observed beyond 30 min. This observation was confirmed by the increase of gypsum peak ($CaSO_4$ dihydrate) in the XRD pattern of treated biosolids at increasing extraction time (data not shown). Other studies [58,59] have also reported consistently low Ca extraction (3–15%) with H_2SO_4 regardless of the concentration owing to the poor solubility of $CaSO_4$ hydrates in water [60]. Cd, Ni, and Cu extraction rates increased with increasing acid concentration, and the influence of acid concentration was significant ($p < 0.05$) on the extraction of Cu and Cd than Ni. However, Cu extraction reached equilibrium faster than Cd, and longer extraction time appeared to favour Cd extraction at higher acid concentrations, which agreed with the findings of Safarzadeh et al. [40]. The improvement in Ni extraction with increasing acid concentration from 1% to 5% was 13% in the first 30 min and increased to 20% after 180 min of extraction, similar to the observation reported by Stylianou et al. [32]. Cd and Ni are mainly present as reducible fractions in biosolids strongly linked to carbonates, and higher acid concentration can increase the dissolution rate of carbonate-containing matrix [28]. Cu can easily form complexes with organic matter due to the high stability constant of organic Cu compounds [61]. Thus, the improved organic matter oxidation at high acid concentration likely favoured the extraction of Cu. The metal dissolution process was strongly influenced by the acid concentration and extraction time due to the differences in the amount of available H^+ and the competitive formation of respective metal sulphate film that slowed down the extraction [62].

3.1.3. Effects of temperature

The influence of temperature on the metal extraction rate is illustrated in Fig. 3. The regression analysis and ANOVA of the process parameter can be found in Table SI3. The influence of temperature on the metal extraction profile was different for each metal. Similar to the effect of acid concentration, the leaching temperature had little to no influence ($p > 0.05$) on the extraction of Na, K, Mg and Zn, whereas temperature played a foremost role in the extraction of Cu, Cd and Ni. The maximum extraction efficiency of Na, K, Mg and Zn ranges from 80% to 100% at all temperatures. Zn and Mg had the highest extraction efficiency of over 99% and had the least variation with temperatures, indicating high extraction stability in H_2SO_4 at the investigated conditions. Ambient temperature (25 °C) slightly outperformed higher temperatures for AAEMs (excluding Ca) removal, suggesting that the metals are available as salts unbounded to the biosolids organic matrix, which would otherwise require harsh pre-treatment conditions to dissociate [53]. The optimum extraction temperature for Ni (76%) and Cd (99%) was 100 °C, whereas it was 63 °C for Cu (85%). The influence of extraction time was more prominent on Ni than Cu and Cd at all temperatures. For instance, Ni extraction at 100 °C reached 50% in 20 min whereas it took around 180 min to reach the same 50% extraction at 25 °C. Meanwhile, the marginal increase in Cd extraction (~10–15%) at all temperatures was similar up to the first 60 min, beyond which the extraction rate waded stronger at 25 °C while it steadily decreased at 100 °C and the extraction converged at 80% at 180 min. Other researchers [40,50,63] found no remarkable influence of time on Cd extraction with H_2SO_4 at 25–60 °C with reported maximum extraction of ~95% in < 15 min. However, in the current study, the extraction temperature was up to 100 °C and the time extended to 180 min; hence the effect of time on Cd extraction at different temperatures was obvious. The effect of temperature on Cu extraction was notable. No earlier work studied the effect of temperature up to 100 °C on Cu dissolution from biosolids. In the current study, Cu extraction increased (from 73% to 85%) with the increase in temperature from 25° to 63°C. However, a further increase in temperature to 100 °C dropped Cu extraction to 35%. The decrease in Cu extraction at 100 °C could be attributed to the selective displacement of Cu from $CuSO_4$ in solution by Fe. Iron extraction was very low at 25 °C (30%), which increased to 50% at 63 °C and reached almost 100% at 100 °C (data not shown). Biosolids used in this study had over 10-fold more Fe (15134 mg/kg) than Cu (1240 mg/kg), and Fe is more reactive than Cu. The displacement reaction (Eq. 9) was spontaneous and catalysed by heat and H_2SO_4 at 100 °C [64]. Also, dissolved Cu can participate in the oxidation of ferrous to ferric at high temperatures to precipitate as Cu-ferrite, thereby limiting Cu extraction [65].

$$CuSO_{4(aq)} + Fe_{(s)} \rightarrow FeSO_{4(aq)} + Cu_{(s)} \quad (9)$$

Distinct from other metals, the Ca extraction rate increased in the first 10 min and then plummeted up to 30 min; after that, the extraction rate became relatively constant at all temperatures. The rapid extraction of Ca in the first 10 min was attributed to the removal of water-soluble and acid-exchangeable Ca ions; thereafter, Ca reacted with H_2SO_4 and formed $CaSO_4$, which exhibited retrograde solubility in water at higher temperatures [60]. XRD analysis of the treated biosolids (Fig. SI1) showed that aside from silica, $CaSO_4$ hydrates (bassanite and gypsum)

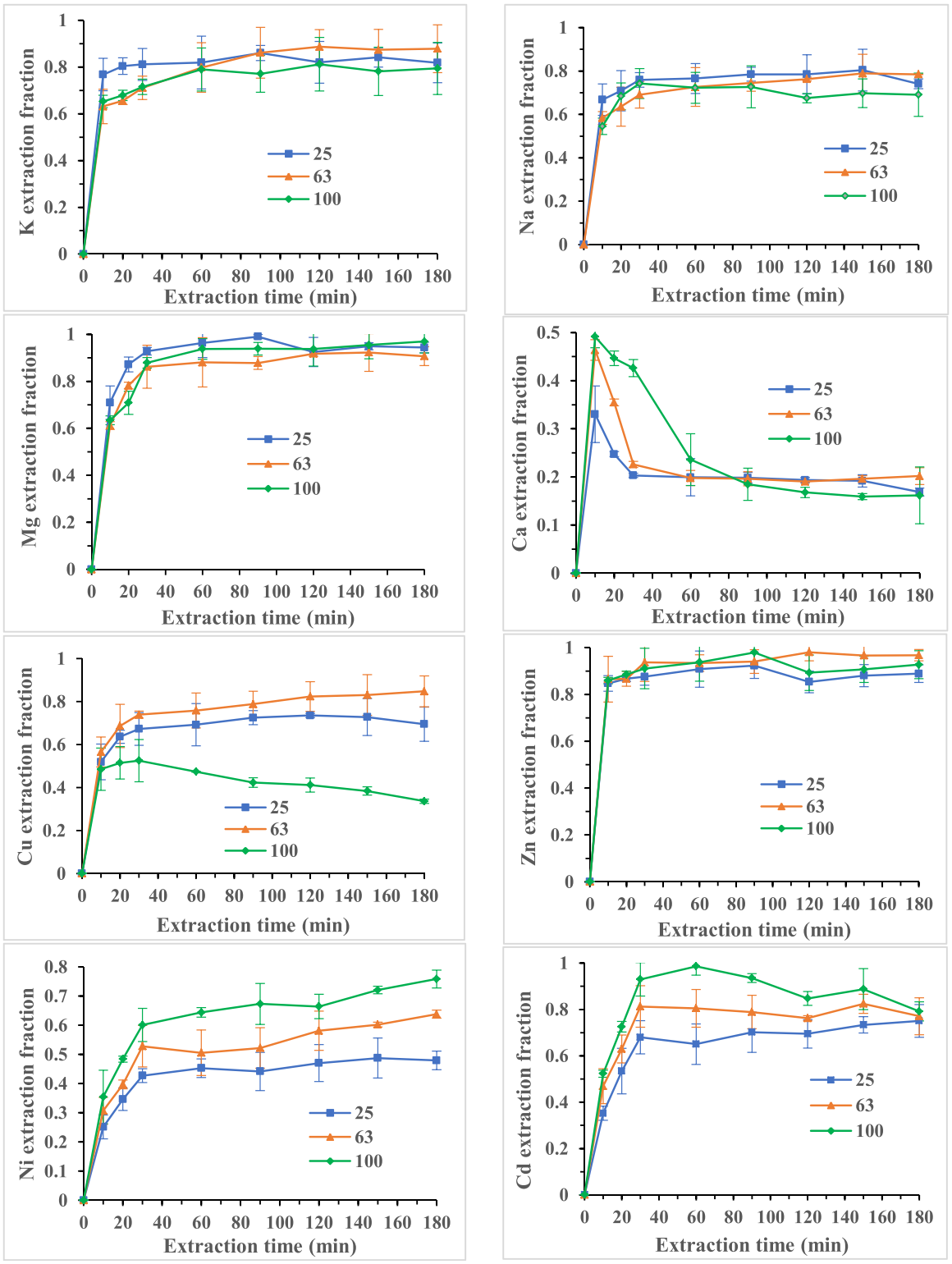

Fig. 3. Effects of temperatures on the extraction rate of AAEMs and controlled HMs in biosolids at 3% H_2SO_4, 600 rpm and 1:10 (g/ml S/L).

were the major mineral phases in the treated biosolids. The absence of other AAEMs sulphates corroborates their high dissolution reaching 85–100% extraction at all temperatures.

3.2. Leaching kinetics

The leaching process observed in this study can be described as a multi-component heterogeneous reaction of several metals and H_2SO_4 at the same time. The reaction rate depends on many factors, including solid surface morphology, surface reactivity, solid activity, and possible phase transfer mechanism [66]. The leaching of AAEMs and Zn was so rapid that it was not possible to fit the shrinking core kinetic models with their extraction rate. This phenomenon was also evident from the inconsequential influence and statistical insignificance ($p > 0.05$) of the leaching parameters (temperature, acid concentration, and time) on AAEMs and Zn extraction (Fig. 2 and 3) Based on the negligible effect of

stirring speeds on all metals extraction (Fig. 1), it was obvious that their extraction kinetics were not limited by external mass transfer and had no effects on the global rate. Therefore, the apparent rate was described either by internal mass transfer (product layer diffusion effects) or surface chemical reaction by fitting Ni, Cd and Cu extraction data to Eqs. 4 and 5 (Fig. SI3(A) and SI3(B), respectively). A satisfactory fitting was observed for extraction data from 0 to 30 min, while no fitting was found for extraction data beyond 30 min for the three metals. The product layer diffusion model was a better fit for Cu extraction data (R^2 >0.94) than the surface chemical reaction model (R^2~0.85). For Ni, both the diffusion model and the surface reaction model appeared to have a good fitting with its experimental data (R^2 >0.94). However, the product layer diffusion model provided a stronger fit with a higher R^2 value of 0.99 and near-zero intercept. Similarly, Cd extraction data had a good fit with both models (R^2 >0.95); however, the surface reaction model gave a stronger fit (R^2 = 0.99). Studies reporting the extraction kinetics of HMs removal from biosolids are scarce. Lee et al. [67] observed a mixed model by combining Eqs. (3)–(5) offered a better description of HMs extraction kinetics from biosolids.

In estimating the leaching activation energy (E_a), only Ni and Cd extraction followed the Arrhenius temperature-dependent rate correlation (Eq. 6) with k_d and k_r increasing with extraction temperatures. For Ni, the plot of ln k_d versus 1000/T (Fig. SI3(C)) gave a strong linear fitting (R^2 >0.999), and for Cd, the plot of ln k_r versus 1000/T (Fig. SI3 (D)) gave an R^2 value of 0.987. Cu extraction kinetics did not follow the Arrhenius rate law; therefore, the leaching E_a for Cu cannot be determined from the investigated pre-treatment conditions. From the slope of the Arrhenius plots, a leaching E_a of 10.020 kJ/mol was estimated for Ni and 7.371 kJ/mol for Cd. The small E_a for Ni extraction is characteristic of a diffusion-controlled process [39,67], which corroborated the stronger fit of the diffusion model with its extraction data. However, the 7.371 kJ/mol E_a for Cd leaching was rather small for a chemical-reaction dominated process; higher E_a (>30 kJ/mol) is typical for a chemical reaction driven process [48,50,67]. Notwithstanding, studies have shown that some chemically controlled processes can have unusually low E_a. For instance, Meshram et al. [68] obtained E_a values of 7.6–13.5 kJ/mol for the H_2SO_4 leaching of rare earth metals from spent batteries for a process identified to be well fitted by a surface chemical reaction model (R^2 ≥0.998). Also, Habbache et al. [49] observed that Cu dissolution from CuO catalyst material using HCl and H_2SO_4 gave < 30 kJ/mol as E_a for the process determined to be controlled by surface chemical reaction phenomena. It appears that the rate-controlling mechanism of heterogeneous dissolution reactions is sometimes predicted from the kinetic equation plots rather than from the E_a value. Although in many cases, both variables can convey corroborating mechanistic information [69]. Comparing the E_a value obtained in this study with extant literature, Lee et al. [67] estimated 7.35 kJ/mol as leaching E_a for Cd extracted in HNO_3 from biosolids. The E_a of diffusion dominated Ni leaching from metal ores and hazardous materials has been reported over a wide range of 9–60 kJ/mol [39,41,48,50]. The estimated Ni leaching E_a (10.02 kJ/mol) in this study was within the lower end of the range.

3.3. Characterisation of treated biosolids

3.3.1. Ultimate and proximate analyses

The effect of pre-treatment on the ultimate and proximate properties of biosolids is summarised in Table 1. A general increase in atomic C, H, and O was observed in all treated feeds relative to the raw feed. However, pre-treatment with 1–5% acid at 63–100 °C caused a decrease in O/C ratio and a slight increase in C/H ratio (Fig. SI4(B)), which improved fuel and energy recovery potential of the feed materials. The increase in HHV from 14.59 MJ/kg in raw biosolids to 16.05–19.16 MJ/kg in treated samples was attributed to reduction in ash contents [70]. Also, the pre-treatment preserved the N content in all treated samples, which may benefit their nutrient value for land application [71]. The

Table 1
Effects of pre-treatment on biosolids ultimate and proximate properties.

Pre-treatment conditions			Proximate analysis (wt% d.b)[a]				Ultimate Analysis (wt% d.a.f)[b]						HHV (MJ/kg)[c]	Solids recovery (%)
A (°C)	B (% v/v)	C (min)	M	VM	FC	Ash	C	H	N	S	O			
Raw biosolids			0.76 ± 0.17	56.99 ± 0.35	11.98 ± 0.11	30.31 ± 0.69	41.73 ± 0.22	4.62 ± 0.18	6.15 ± 0.20	1.27 ± 0.06	15.85 ± 0.09		14.59 ± 0.15	–
Effects of temperature														
25	3	30	2.17 ± 0.18	62.45 ± 0.15	19.93 ± 0.33	15.45 ± 0.30	48.64 ± 0.95	5.54 ± 0.23	6.98 ± 0.18	1.65 ± 0.04	22.26 ± 1.39		19.16 ± 0.76	74.72 ± 2.36
63	3	30	3.00 ± 0.05	62.40 ± 0.42	17.40 ± 0.41	17.20 ± 0.04	46.33 ± 1.17	5.12 ± 0.28	6.74 ± 0.30	1.81 ± 0.12	22.80 ± 1.64		17.79 ± 0.89	65.49 ± 3.61
100	3	30	1.93 ± 0.69	61.44 ± 0.45	13.02 ± 0.30	23.60 ± 0.54	43.52 ± 3.92	4.70 ± 0.43	6.19 ± 0.35	3.09 ± v 0.21	18.91 ± 4.50		16.05 ± 2.33	54.62 ± 3.45
Effects of acid concentration														
63	1	30	3.03 ± 0.00	61.22 ± 0.55	17.56 ± 0.56	18.19 ± 0.00	47.21 ± 2.16	4.90 ± 0.57	7.06 ± 0.13	1.56 ± 0.12	21.07 ± 2.74		17.86 ± 1.69	70.36 ± 2.86
63	3	30	3.00 ± 0.05	62.40 ± v 0.42	17.40 ± 0.41	17.20 ± 0.04	46.33 ± 1.17	5.12 ± 0.28	6.74 ± 0.30	1.81 ± 0.12	22.80 ± 1.64		17.79 ± 0.89	65.49 ± 3.61
63	5	30	2.34 ± 0.38	64.00 ± 0.98	17.07 ± 0.33	16.59 ± 0.26	45.31 ± 0.32	4.72 ± 0.16	6.47 ± 0.12	2.64 ± 0.20	23.84 ± 0.55		17.07 ± 0.29	62.84 ± 2.19

increase in S contents in TB relative to the RB can be attributed to the residual S from H_2SO_4 despite post-treatment water washing carried out or due to the formation of sulphides by the oxidising action of H_2SO_4 on metals, particularly at higher treatment temperatures and acid concentrations [72]. The severity of the pre-treatment conditions affects the proximate properties particularly, the ash and fixed carbon (FC) contents ((Fig. SI4(A)). At low severity conditions (25 °C and 3% acid), ash content was reduced by 50% from 30.31 in RB to 15.45 wt%, while volatile matter (VM) increased from 56.99 wt% to 62.45 wt%. The increase in VM observed in all treated feeds suggested that the pre-treatment conditions were mild and did not cause noticeable organic matter degradation. However, the harshest treatment conditions (100 °C and 5% acid) caused the least increase in VM (59 wt% (data not shown)). It was observed that the increase in temperature increased the ash content, whereas the increase in acid concentration decreased the ash content (Table 1). Therefore, a higher acid concentration and lower temperature combination would give the best de-ashing outcome. FC increased in all treated biosolids (13–20 wt%) from 12 wt% in RB as labile carbon was likely transformed to recalcitrant carbon during the pre-treatment. The solids recovery decreased with increasing severity levels of the pre-treatment, with the highest recovery (74.72%) observed at the mildest condition.

A – Temperature; B – Acid concentration; C – Time; [a]dry basis; [b]dry ash-free; [c]estimated by the correlation of Channiwala and Parikh [70] using $HHV(MJ/kg) = 0.3491C + 1.1783H + 0.1005S - 0.1034O - 0.0151N - 0.0211Ash$.

3.3.2. Functional groups of raw and treated biosolids and their biochar

The FTIR spectra of raw and treated biosolids (Fig. SI5) and their interpretation are provided in Supplementary SI5. The analysis was used to assess the compositional stability of the biosolids after acid treatment and to understand the possible role of the functional groups in the metal removal process. Biosolids contain organic matter with diverse chemical groups, and metals extraction with leaching solvents can be closely related to the abundance and type of functional groups [73]. Insights into the leaching mechanisms that can involve the deprotonation of carboxylic O–H and hydroxylic O–H groups to release H^+, aiding the desorption of metals from biosolids is given in Supplementary SI9. Most of the compounds signatures in RB are preserved in the treated feeds indicating very mild alterations of the biochemical compositions following acid treatment. The sample treated at 25 °C and 63 °C did not show any obvious difference in their spectra compared to RB (Fig. SI5). However, for the sample treated at 100 °C and 5% acid, organic constituent vibrations in the waveband 900–650 cm^{-1} became fuzzy, indicating possible molecular bond distortion of substituted C–H groups. A remarkable increase in the intensity of the Si-O peak (980 cm^{-1}) was observed in the spectra of all treated samples compared to RB due to the relatively higher silica concentration in treated feeds (corroborated by XRF result in Fig. 5). Likewise, RBB and TBB had similar functional groups indicating that the pre-treatment did not impact the surface chemistry of the TB and their resulting biochar (Fig. SI6).

3.3.3. Structural morphologies and surface area

SEM images of raw and acid-treated samples are shown in Fig. SI7. Noticeable differences in the surface morphology were observed at mid to high temperature treated samples (Fig. SI7(D–F)). RB image (Fig. SI7 (A)) showed a slit-like flat layered surface, and this layered surface became disordered when acid was added to the biosolids samples. Acid treatment caused some structural changes due to diffusion, which resulted in mild to strong pore openings. No noticeable alteration in surface morphology was observed for the room-temperature treated samples (Fig. SI7(B) and (C)) despite excellent metals and minerals removals. This observation indicated that the treatment predominantly leached free and inorganic-bounded metals and was insufficient to create inner pores within the organic matrix. Higher treatment temperature changed the morphology of the samples with emerging porous structures (Fig. SI7(D–F)). The surface appearance of TB showed fine whitish-grey crystals covering attributable to the formation of $CaSO_4$ hydrates and $PbSO_4$, which are the two major mineral phases poorly leached by H_2SO_4 [74]. However, despite these mild to strong morphological changes in the treated feeds, their BET specific surface areas (2.059–3.048 m^2/g) and pore volumes (0.0127–0.0226 cm^3/g) were similar to the RB (2.559 m^2/g and 0.0147 cm^3/g). The pore size distribution revealed that mainly mesoporous (average pore width = 7.449 nm) are present in RB, and the width of the pores increased slightly in treated feeds. The pre-treatment conditions employed in the current study was insufficient to cause an appreciable increase in surface areas and pore volumes.

3.3.4. Thermal decomposition behaviour

The thermal decomposition behaviour of biosolids following acid treatment was studied, and the thermographs are shown in Fig. 4. From the DTG curve (Fig. 4(B)), six clear peaks (I–VI) at 80, 155, 320, 360, 465, and 705 °C were observed in the RB degradation profile. Peak I and peak II are attributed to the loss of moisture and light volatiles, respectively. Peaks III–V represent the major mass loss due to the decomposition of organic matter, and peak (VI) is ascribed to the loss of inorganics, usually carbonates. Pre-treatment temperatures influenced the thermal decomposition behaviour of TB. For instance, peak II and peak VI associated with the decomposition of light volatiles and inorganics completely disappeared in all TB. This observation suggested that acid treatment of biosolids, irrespective of severity conditions, caused a loss of light volatiles (leachable organics) and minerals. Pre-treatment facilitated the thermal degradation of biosolids components with a higher weight loss rate, similar to the observations reported in previous studies [14,44,46]. The peaks associated with organics decomposition persisted in all treated samples but at different intensities. For example, S5 and S2 had higher weight loss rates, but the maximum degradation peak shifted to a lower temperature (290 °C) for S5 and higher temperature (360 °C) for S2 compared to 305 °C for RB. Also, the increased devolatilisation of S5 and S2 resulted in low residues generation compared to RB and S4 (Fig. 4(A)). However, the DTG profile of S4, obtained at 100 °C and 5% H_2SO_4, displayed a different decomposition pattern having a lower degradation rate, as the maximum degradation temperature increased by 60 °C compared to RB. Therefore, pre-treatment at 100 °C may be undesirable as it caused significant components hydrolysis, which compromised the pyrolysis performance. Shao et al. [43] also observed that demineralisation of biosolids using 2 M HCl and 60 °C hindered the degradation of organic macromolecules due to changes in the biosolids structure caused by the pre-treatment.

3.4. Overall implications of acid pre-treatment on biosolids

3.4.1. Biosolids grade

The XRF analysis of treated biosolids samples is presented in Fig. 5, and their residual metals concentration is summarised in Table SI4. The major mineral phase identified in the TB can be found in the XRD pattern (Fig. SI1). From both XRF and XRD analyses, the main minerals bearing elements in TB were Ca, Si, Al, Fe, and P, and their concentration intensities were impacted by pre-treatment conditions (Fig. 5). Trace amounts of other metals, including Cu, Zn, Ni, Cr, and Mn, were also detected in the treated samples at different concentration intensities (Fig. SI8). The overall observations are consistent with temperature, acid concentration and extraction time effects on the metals extraction efficiency (Fig. 1–3). All the TB met the C1-grade biosolids HMs concentration threshold except for Cu (Table SI4). The maximum Cu extraction was 95% at 63 °C and 5% acid, corresponding to a residual Cu concentration of 241.8 mg/kg in the TB from 1239.81 mg/kg in the RB. Therefore, more than 95% Cu removal is required to achieve the 100 mg/kg Cu concentration threshold for C1-grade biosolids. The required Cu concentration could be achieved using > 5% H_2SO_4 and 63 °C or higher temperature (63 °C<T < 100 °C) and 3% H_2SO_4 or

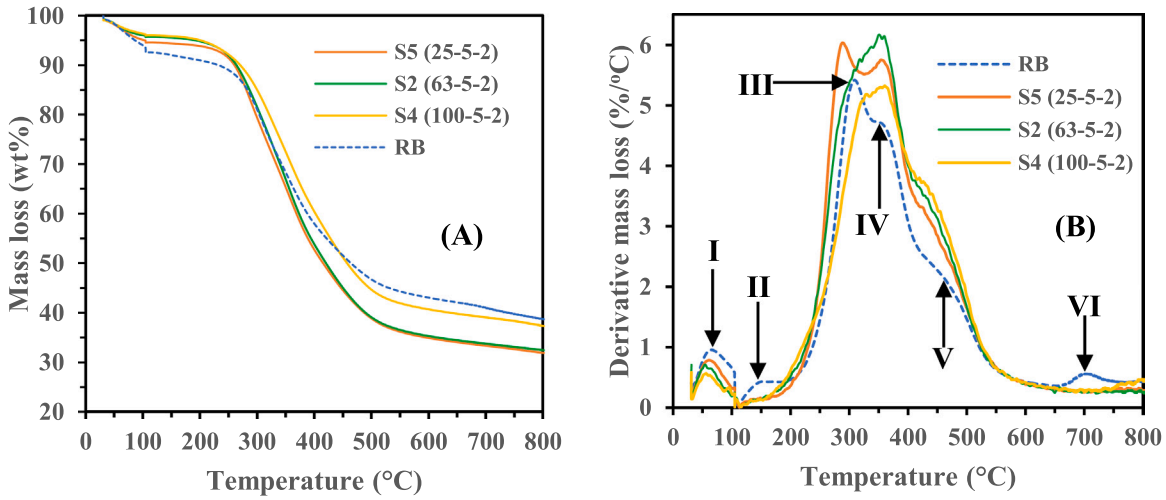

Fig. 4. Thermal degradation behaviour of raw and acid-treated biosolids obtained at different pre-treatment conditions (A) TGA profile (B) DTG profile.

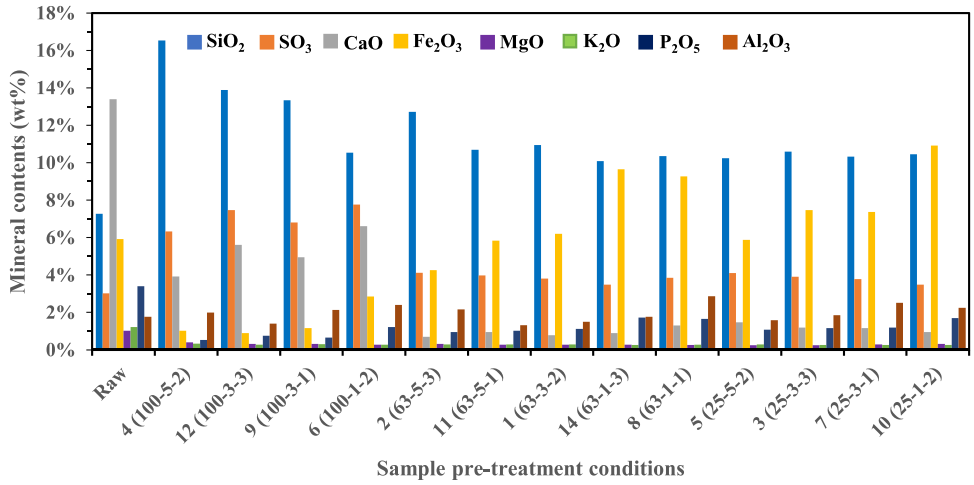

Fig. 5. Relative minerals composition in raw and treated biosolids.

using a two-step extraction at mild pre-treatment conditions or using acidified $FeCl_3$, $Fe_3(SO_4)_2$ and H_2O_2 [29,75,76]. Cu extraction is influenced by the oxidation-reduction potential of the extracting solvents rather than acidic pH alone [76,77]. At all conditions studied, 100% removal of the HMs was not observed; a modest extraction of 70–95% was achieved at the optimum conditions. The retained HMs in the TB will likely be present as organic-bounded and residual fractions, which will be highly resistant to lixiviation when applied to soil [34,78].

3.4.2. *Nutrient status*

The major nutrient elements in biosolids are N, P, K and acid leaching can solubilise the components that enrich biosolids of these elements. Except for N, which is modestly preserved in the TB (Table 1), there was a reduction in the P and K contents after the acid leaching, even at the mildest conditions. For instance, the total P in raw biosolids was 1.5 wt%, and it was reduced to 0.8 wt% in biosolids treated at 25 °C and 1% H_2SO_4. Consequently, the H_2SO_4 treatment altered the N:P:K ratio in the TB relative to the RB, influencing their agronomic value [28]. The joint use of ferric salt or H_2O_2 alongside dilute H_2SO_4 can effectively reduce P solubilisation through the co-precipitation of P as ferric phosphate and Fenton oxidation reaction [28,75]. On the other hand, the pre-treatment could facilitate the production of nutrient modified biosolids for targeted agricultural land applications. Kokkora et al. [79] suggested that the fertilising requirement of biosolids depends largely on the specific agricultural soil's nutrient demand, and excessive levels of these highly labile nutrients, particularly P, can have negative environmental implications in some cases.

3.4.3. *Dewaterability and conditioning*

The acid treatment of biosolids lowered the pH from 6.8 to < 2, which may affect the conditioning and dewaterability of the TB. We observed that the mechanical dewatering of the acid-treated biosolids via centrifugation was not altered compared to the raw biosolids at the same conditions. Chen et al. [80] found that pH < 3 favoured the centrifugal dewatering efficiency of H_2SO_4 treated sludge through a monotonic decrease in sludge volume. For instance, about 50% reduction in sludge volume was observed when the pH declined from 6.8 (raw sludge) to 1.5 (treated sludge). Similarly, Beauchesne et al. [28] observed that sludge treatment with H_2SO_4 and ferric/H_2O_2 at lower pH enhanced dewaterability through improvement in flocs quality and reduction in capillary suction time. The emulsification of soluble proteins and lipids components following the destruction of extracellular polymeric substances in the biosolids at acidic pH promoted particles agglomeration and rheological behaviour, mainly improving dewaterability to a larger extent [80–82]. Except where the production of activated char via pyrolysis is desired, the treated biosolids demands post-treatment conditioning before land application or thermochemical conversion to biochar. pH correction via water or alkali washing is a

common approach; however, a huge volume of aqueous waste stream is generated. Lime conditioning of the treated biosolids can correct the pH to the desired level while concurrently replenishing the biosolids of lost nutrients.

3.4.4. Techno-economic and leachate management

The techno-economic viability of the acid leaching process and land applications of the treated products is necessary to facilitate the widespread adoption of this integrated approach to biosolids management. Few studies have overviewed the techno-economic status of biosolids leaching for HMs removal [26,30,83]. However, there is a paucity of information on the economics of acid leaching hybridised with pyrolysis to produce quality biosolids and biochar suitable for land application. Lastly, the management of the acidic aqueous stream containing dissolved metals is a typical limitation of acid pre-treatment. Suggestions in the literature include returning to WWTPs for tertiary treatment, alkali neutralisation, metals recovery via precipitation, adsorption, electrowinning, and membrane separation [62,84–86]. However, depending on the diversity of the metal components and their concentration in the stream, some of these techniques can be ineffective, expensive or even generate residual wastes. A close-loop hydrometallurgical option involving concentrating the stream through reuse and recycling, purifying the concentrated stream, and recovering valuable metals could be more attractive and should be explored in detail [87].

3.5. Effect of pre-treatment and pyrolysis on biosolids biochar: the fate of metals

The metals (AAEMs and HMs) contents in raw and treated biosolids-derived biochar (i.e., RBB and TBB, respectively) are given in Table 2. The contents of the metals in the parent materials (i.e., RB and TB) were also provided to understand the effect of pre-treatment and subsequent pyrolysis on the metals' retention in the biochar. Biochar yield from TB (35.59 wt%) was lower than that from RB (50.68 wt%) due to the low ash content in TB. Total AAEMs load in TB was 2.45 times lower than RB, equivalent to a 60% AAEMs removal during the pre-treatment. Pyrolysis of both RB and TB further increased the AAEMs concentration considerably. The produced biochar had AAEMs concentrations of ~133000 and ~54000 mg/kg for RBB and TBB, respectively. High levels of AAEMs and other ash components in biochar are undesirable as they can decrease the biochar surface areas, limit microporous structure formation and activation performance, which may hinder their application in catalysis and adsorption [88]. Moreover, the high ash content in biochar can reduce the carbon sequestration potential and calorific value [7,14], thereby lowering biochar attractiveness for land application and energy recovery. Therefore, biosolids pre-treatment before pyrolysis can produce quality biochar with low ash and AAEMs contents and high fixed carbon relative to RBB; however, at the cost of biochar yield.

Pyrolysis concentrates HMs in the biochar due to considerable mass reduction of the biosolids feed, equivalent to about 50% and 65% reduction for RB and TB, respectively (Table 2). Hence, the metals concentrations in both RBB and TBB increased by at least 1.5-fold compared to the concentration in their respective biosolids feed. The total concentration of all metals except Pb decreased drastically by at least 25% in TBB compared to RBB, indicating that the biosolids pre-treatment effectively lowered HMs in the resulting biochar. The similar Pb concentration in both RBB and TBB was due to the very low extraction of Pb during the biosolids pre-treatment. However, the retention rate for all metals in RBB was lower than that for TBB due to the higher biochar yield in RB that enhanced the metal dilution rate. The metal component with the highest and lowest MRF was not the same for both RBB and TBB, which can be linked to different removal efficiency of the metals during pre-treatment and the chemical form of the residual metals in the TB. For instance, Cr had the highest MRF (1.980) in RBB, which shifted to Cu (3.217) in TBB. Similarly, As had the lowest MRF (1.462) in RBB, and it was Pb (2.145) for TBB. This observation suggests that biosolids pre-treatment can help to selectively lower or enrich a metal of interest in the resultant biochar for targeted applications. Apart from the highly volatile HMs such as As and Cd [19,20], the recovery rate of other metals was > 80%, indicating that all the HMs are immobilised almost completely in the char. Notably, the metals recovery was slightly higher in TBB than RBB due to the higher stability of the residual metals in the TB following the removal of the leachable metals during pre-treatment. The similar recoveries of Cr, Cu, Ni, and Zn in both char products were credited to the metals' relatively lower mobility, which promoted their transformation to residual fraction at pyrolysis conditions [89]. The overall observation suggests that pre-treatment can influence the migration characteristics of HMs during biosolids pyrolysis.

Although the concentration of the metals in both RBB and TBB were within the lower limits suggested by the International Biochar Initiative guideline [90], only TBB met the requirement of C1-grade material HMs concentration but was limited by Cu. However, the ecological risks with the residual HMs in the biochar can be highly reduced. Studies involving biosolids biochar soil trials demonstrate that the metals are immobile with low leaching toxicity and plant availability [91,92]. Therefore, pyrolysis of de-metallised biosolids can produce high-quality biochar and effectively inhibit the transport of HMs from the biochar during land application.

Table 2
Fate of metals in biosolids and their derived biochar.

Samples	C1-grade[a]	RB	TB	RBB	TBB				
Biochar yield (wt%)				50.68	35.59				
HMs concentration (mg/kg)						**MRF**		**R (%)**	
						RBB	**TBB**	**RBB**	**TBB**
As	20	3.64 ± 0.78	1.69 ± 0.16	5.32 ± 1.65	3.98 ± 0.74	1.462	2.355	74.09	83.34
Cd	1	1.87 ± 0.21	0.57 ± 0.12	2.86 ± 0.84	1.33 ± 0.17	1.529	2.333	77.49	83.04
Cr	400	20.65 ± 2.31	10.36 ± 1.36	40.88 ± 9.85	28.98 ± 4.51	1.980	2.797	~100	~100
Cu	100	1239.81 ± 341.13	192.60 ± 10.31	2335.19 ± 217.59	619.62 ± 96.07	1.884	3.217	95.48	100
Ni	60	35.40 ± 1.37	11.73 ± 1.89	58.28 ± 13.85	29.39 ± 8.89	1.646	2.506	83.44	89.17
Pb	300	23.60 ± 1.84	19.71 ± 1.14	41.81 ± 5.15	42.28 ± 6.05	1.772	2.145	89.80	76.34
Zn	200	1075.14 ± 124.98	76.24 ± 6.87	2045.21 ± 175.01	209.47 ± 78.57	1.902	2.748	96.41	97.78
Total AAEMs (g/kg)		61.74 ± 2.28	25.19.32 ± 1.27	133.21 ± 12.33	53.66 ± 4.89				
Ash contents (wt%)		30.31 ± 0.69	17.20 ± 0.04	53.57 ± 1.25	43.40 ± 2.17				
FC (wt%)		11.98 ± 0.11	17.40 ± 0.41	19.47 ± 1.46	25.53 ± 1.89				

[a] Least contaminant grade biosolids as described in Victoria EPA biosolids guidelines [5]. RB – Raw biosolids; TB – Treated biosolids; RBB – Raw biosolids biochar; TBB – Treated biosolids biochar; MRF – Metals retention factor; R – Metal recovery.

4. Conclusions

Mild H_2SO_4 pre-treatment of biosolids was carried out to remove deleterious HMs and ash-forming metals (AAEMs), resulting in high-grade biosolids and biochar. The extraction profiles of all metals were very similar and rapid, reaching equilibrium in 30 min. About 80–90% of AAEMs except Ca were removed during the pre-treatment, and this extraction rate was not largely influenced by leaching temperature and acid concentration. The formation of $CaSO_4$ hydrates limited Ca extraction to 20% at all pre-treatment conditions. The maximum extraction of 95%, 95% and 75% was recorded for Cu, Cd, and Ni, respectively, at different optimum conditions. Ni extraction was controlled by the product layer diffusion mechanism with a leaching activation energy of 10.02 kJ/mol, while the surface chemical reaction model described Cd extraction. Acid pre-treatment at the mildest condition reduced the ash content in raw biosolids by 50% but did not alter important physicochemical properties, such as surface chemical groups and surface morphology. Pre-treatment enhanced biosolids pyrolysis behaviour with a higher weight loss rate and low solid residues generation than raw biosolids. Biosolids pre-treatment prior to pyrolysis further reduced the total HMs concentration in resultant biochar by at least 50% albeit, at the expense of biochar yield. The decontamination of biosolids and their derived char through mild H_2SO_4 leaching could effectively solve the increasing challenge of biosolids land application.

CRediT authorship contribution statement

Ibrahim Gbolahan Hakeem: Conceptualization, Methodology, Formal analysis, Investigation, Software, Writing – original draft, **Pobitra Halder:** Validation, Visualization, Data curation, Writing – review & editing. **Mojtaba Hedayati Marzbali**: Visualisation, Validation, Writing – review & editing. **Savankumar Patel**: Resources, Writing – review & editing. **Nimesha Rathnayake:** Writing – review & editing. **Aravind Surapaneni:** Resources, Supervision. **Graeme Short**: Supervision. **Jorge Paz-Ferreiro**: Supervision, Writing – review & editing. **Kalpit Shah:** Conceptualization, Validation, Supervision, Project administration.

Declaration of Competing Interest

The authors declare that they have no known competing financial interests or personal relationships that could have appeared to influence the work reported in this paper.

Acknowledgement

This work is supported by the School of Engineering, RMIT University, Australia and the ARC Biosolids Industrial Transformation Traning Centre at RMIT University. The first author is indebted to RMIT University, Australia for the postgraduate scholarship recieved. The authors would like to thank Stephen Grist and Nadia Zakhartchouk for the assistance received with the ICP-MS, FTIR and XRF characterisation. The use of BET equipment in the Advanced Porous Materials Lab and SEM instrument in the Microscopy and Microanalysis Facility at RMIT University is acknowledged.

Appendix A. Supporting information

Supplementary data associated with this article can be found in the online version at doi:10.1016/j.jece.2022.107378.

References

[1] J. Paz-ferreiro, A. Nieto, A. Méndez, M.P.J. Askeland, G. Gasco, Biochar from biosolids pyrolysis: a review, Int. J. Environ. Res. Public Health 15 (2018) 1–16, https://doi.org/10.3390/ijerph15050956.

[2] A. Zaker, Z. Chen, M. Zaheer-Uddin, Catalytic pyrolysis of sewage sludge with HZSM5 and sludge-derived activated char: a comparative study using TGA-MS and artificial neural networks, J. Environ. Chem. Eng. 9 (2021), 105891, https://doi.org/10.1016/J.JECE.2021.105891.

[3] R.J. LeBlanc, P. Matthews, R.P. Richard, Global atlas of excreta, wastewater sludge, and biosolids management: moving forward the sustaianble and welcome uses of a global resource, United Nations Human Settlements Programme, UN-HABITAT, P. O. Box 30030, Nairobi 00100, Kenya, 2009.

[4] ANZBP, Biosolids production in Australia – 2019, 2020. https://doi.org/https://www.biosolids.com.au/guidelines/australian-biosolids-statistics/.

[5] EPA Victoria, Guidelines for Environmental Mangement: Biosolids Land Application, Southbank, Victoria 3006, Australia, 2004.

[6] M. Abis, W. Calmano, K. Kuchta, et al., Innovative technologies for phosphorus recovery from sewage sludge ash, Detritus 1 (2018) 23–29.

[7] S. Patel, S. Kundu, P. Halder, N. Ratnnayake, M.H. Marzbali, S. Aktar, E. Selezneva, J. Paz-Ferreiro, A. Surapaneni, C.C. de Figueiredo, A. Sharma, M. Megharaj, K. Shah, A critical literature review on biosolids to biochar: an alternative biosolids management option, Rev. Environ. Sci. Biotechnol. 19 (2020) 807–841, https://doi.org/10.1007/s11157-020-09553-x.

[8] I. Fonts, G. Gea, M. Azuara, J. Ábrego, J. Arauzo, Sewage sludge pyrolysis for liquid production: a review, Renew. Sustain. Energy Rev. 16 (2012) 2781–2805, https://doi.org/10.1016/j.rser.2012.02.070.

[9] P. Manara, A. Zabaniotou, Towards sewage sludge based biofuels via thermochemical conversion – a review, Renew. Sustain. Energy Rev. 16 (2012) 2566–2582, https://doi.org/10.1016/j.rser.2012.01.074.

[10] S. Patel, S. Kundu, P. Halder, G. Veluswamy, B. Pramanik, Slow pyrolysis of biosolids in a bubbling fluidised bed reactor using biochar, activated char and lime, J. Anal. Appl. Pyrolysis 144 (2019) 1–11, https://doi.org/10.1016/j.jaap.2019.104697.

[11] J.J. Ross, D.H. Zitomer, T.R. Miller, C.A. Weirich, P.J. Mcnamara, Emerging investigators series: pyrolysis removes common microconstituents triclocarban, triclosan, and nonylphenol from biosolids, Environ. Sci. Water Res. Technol. 2 (2016) 282–289, https://doi.org/10.1039/C5EW00229J.

[12] O.S. Djandja, Z.C. Wang, F. Wang, Y.P. Xu, P.G. Duan, Pyrolysis of municipal sewage sludge for biofuel production: a review, Ind. Eng. Chem. Res. 59 (2020) 16939–16956, https://doi.org/10.1021/acs.iecr.0c01546.

[13] R. Chen, X. Ma, Z. Yu, L. Chen, X. Chen, Z. Qin, Study on synchronous immobilization technology of heavy metals and hydrolyzed nitrogen during pyrolysis of sewage sludge, J. Environ. Chem. Eng. 9 (2021), 106079, https://doi.org/10.1016/J.JECE.2021.106079.

[14] H. Nan, F. Yang, L. Zhao, O. Mašek, X. Cao, Z. Xiao, Interaction of inherent minerals with carbon during biomass pyrolysis weakens biochar carbon sequestration potential, ACS Sustain. Chem. Eng. 7 (2018) 1591–1599, https://doi.org/10.1021/ACSSUSCHEMENG.8B05364.

[15] D. Vamvuka, N. Salpigidou, E. Kastanaki, S. Sfakiotakis, Possibility of using paper sludge in co-firing applications, Fuel 88 (2009) 637–643, https://doi.org/10.1016/J.FUEL.2008.09.029.

[16] P. Giudicianni, V. Gargiulo, C.M. Grottola, M. Alfè, A.I. Ferreiro, M.A.A. Mendes, M. Fagnano, R. Ragucci, Inherent metal elements in biomass pyrolysis: a review, Energy Fuels 35 (2021) 5407–5478, https://doi.org/10.1021/ACS.ENERGYFUELS.0C04046.

[17] I.G. Hakeem, P. Halder, M.H. Marzbali, S. Patel, S. Kundu, J. Paz-Ferreiro, A. Surapaneni, K. Shah, Research progress on levoglucosan production via pyrolysis of lignocellulosic biomass and its effective recovery from bio-oil, J. Environ. Chem. Eng. 9 (2021), 105614, https://doi.org/10.1016/j.jece.2021.105614.

[18] A. Nzihou, B. Stanmore, N. Lyczko, D.P. Minh, The catalytic effect of inherent and adsorbed metals on the fast/flash pyrolysis of biomass: a review, Energy 170 (2019) 326–337, https://doi.org/10.1016/J.ENERGY.2018.12.174.

[19] Z. Zhang, R. Ju, H. Zhou, H. Chen, Migration characteristics of heavy metals during sludge pyrolysis, Waste Manag. 120 (2021) 25–32, https://doi.org/10.1016/j.wasman.2020.11.018.

[20] T. Liu, Z. Liu, Q. Zheng, Q. Lang, Y. Xia, N. Peng, C. Gai, Effect of hydrothermal carbonization on migration and environmental risk of heavy metals in sewage sludge during pyrolysis, Bioresour. Technol. 247 (2018) 282–290, https://doi.org/10.1016/j.biortech.2017.09.090.

[21] S. Babel, D. del Mundo Dacera, Heavy metal removal from contaminated sludge for land application: a review, Waste Manag. 26 (2006) 988–1004, https://doi.org/10.1016/j.wasman.2005.09.017.

[22] A. Mulchandani, P. Westerhoff, Recovery opportunities for metals and energy from sewage sludges, Bioresour. Technol. 215 (2016) 215–226, https://doi.org/10.1016/J.BIORTECH.2016.03.075.

[23] S. Gaber, M. Rizk, M. Yehia, Extraction of certain heavy metals from sewage sludge using different types of acids, Biokemistri 23 (2011) 41–48, https://doi.org/10.4314/biokem.v23i1.

[24] C. Naoum, D. Fatta, K.J. Haralambous, M. Loizidou, Removal of heavy metals from sewage sludge by acid treatment, J. Environ. Sci. Heal. Part A. 36 (2001) 873–881, https://doi.org/10.1081/ESE-100103767.

[25] M. Gheju, R. Pode, F. Manea, Comparative heavy metal chemical extraction from anaerobically digested biosolids, Hydrometallurgy 108 (2011) 115–121, https://doi.org/10.1016/J.HYDROMET.2011.03.006.

[26] J.G. Yao, S.Y. Tan, P.I. Metcalfe, P.S. Fennell, G.H. Kelsall, J.P. Hallett, Demetallization of sewage sludge using low-cost ionic liquids, Environ. Sci. Technol. 55 (2021) 5291–5300, https://doi.org/10.1021/acs.est.0c03724.

[27] Junguo He Jian Tang, Xiaodong Xin Tiantian Liu, Removal of heavy metals with sequential sludge washing techniques using saponin: optimization conditions,

kinetics, removal effectiveness, binding intensity, mobility and mechanism, RSC Adv. 7 (2017) 33385–33401, https://doi.org/10.1039/C7RA04284A.
[28] I. Beauchesne, R. Ben Cheikh, G. Mercier, J.F. Blais, T. Ouarda, Chemical treatment of sludge: in-depth study on toxic metal removal efficiency, dewatering ability and fertilizing property preservation, Water Res. 41 (2007) 2028–2038, https://doi.org/10.1016/J.WATRES.2007.01.051.
[29] A. Ito, T. Umita, J. Aizawa, T. Takachi, K. Morinaga, Removal of heavy metals from anaerobically digested sewage sludge by a new chemical method using ferric sulfate, Water Res. 34 (2000) 751–758, https://doi.org/10.1016/S0043-1354(99)00215-8.
[30] A. Pathak, M.G. Dastidar, T.R. Sreekrishnan, Bioleaching of heavy metals from sewage sludge: a review, J. Environ. Manag. 90 (2009) 2343–2353, https://doi.org/10.1016/j.jenvman.2008.11.005.
[31] G. Liu, M.M. Wright, Q. Zhao, R.C. Brown, Hydrocarbon and ammonia production from catalytic pyrolysis of sewage sludge with acid pretreatment, ACS Sustsin. Chem. Eng. 4 (2016) 1819–1826, https://doi.org/10.1021/acssuschemeng.6b00016.
[32] M.A. Stylianou, D. Kollia, K.J. Haralambous, V.J. Inglezakis, K.G. Moustakas, M. D. Loizidou, Effect of acid treatment on the removal of heavy metals from sewage sludge, Desalination 215 (2007) 73–81, https://doi.org/10.1016/j.desal.2006.11.015.
[33] B. Bayat, B. Sari, Comparative evaluation of microbial and chemical leaching processes for heavy metal removal from dewatered metal plating sludge, J. Hazard. Mater. 174 (2010) 763–769, https://doi.org/10.1016/j.jhazmat.2009.09.117.
[34] C.H. Wu, C.Y. Kuo, S.L. Lo, Recovery of heavy metals from industrial sludge using various acid extraction approaches, Water Sci. Technol. 59 (2009) 289–293, https://doi.org/10.2166/wst.2009.859.
[35] Y.C. Kuan, I.H. Lee, J.M. Chern, Heavy metal extraction from PCB wastewater treatment sludge by sulfuric acid, J. Hazard. Mater. 177 (2010) 881–886, https://doi.org/10.1016/J.JHAZMAT.2009.12.115.
[36] J.E. Silva, D. Soares, A.P. Paiva, J.A. Labrincha, F. Castro, Leaching behaviour of a galvanic sludge in sulphuric acid and ammoniacal media, J. Hazard. Mater. 121 (2005) 195–202, https://doi.org/10.1016/J.JHAZMAT.2005.02.008.
[37] S. Yoshizaki, T. Tomida, Principle and process of heavy metal removal from sewage sludge, Environ. Sci. Technol. 34 (2000) 1572–1575, https://doi.org/10.1021/es990979s.
[38] J.I. Mingot, A. Obrador, J.M. Alvarez, M.I. Rico, Acid extraction and sequential fractionation of heavy metals in water treatment sludges, Environ. Technol. 16 (1995) 869–876, https://doi.org/10.1080/09593331608616325.
[39] M. Gharabaghi, M. Irannajad, A.R. Azadmehr, Leaching kinetics of nickel extraction from hazardous waste by sulphuric acid and optimization dissolution conditions, Chem. Eng. Res. Des. 91 (2013) 325–331, https://doi.org/10.1016/J.CHERD.2012.11.016.
[40] M.S. Safarzadeh, D. Moradkhani, M. Ojaghi-Ilkhchi, Kinetics of sulfuric acid leaching of cadmium from Cd-Ni zinc plant residues, J. Hazard. Mater. 163 (2009) 880–890, https://doi.org/10.1016/j.jhazmat.2008.07.082.
[41] V. Houzelot, B. Ranc, B. Laubie, M.O. Simonnot, Agromining of hyperaccumulator biomass: Study of leaching kinetics of extraction of nickel, magnesium, potassium, phosphorus, iron, and manganese from Alyssum murale ashes by sulfuric acid, Chem. Eng. Res. Des. 129 (2018) 1–11, https://doi.org/10.1016/j.cherd.2017.10.030.
[42] Q. Tian, B. Dong, X. Guo, Z. Xu, Q. Wang, D. Li, D. Yu, Comparative atmospheric leaching characteristics of scandium in two different types of laterite nickel ore from Indonesia, Miner. Eng. 173 (2021), 107212, https://doi.org/10.1016/J.MINENG.2021.107212.
[43] J. Shao, R. Yan, H. Chen, H. Yang, D.H. Lee, Catalytic effect of metal oxides on pyrolysis of sewage sludge, Fuel Process. Technol. 91 (2010) 1113–1118, https://doi.org/10.1016/j.fuproc.2010.03.023.
[44] S. Tang, C. Zheng, Z. Zhang, Effect of inherent minerals on sewage sludge pyrolysis: Product characteristics, kinetics and thermodynamics, Waste Manag. 80 (2018) 175–185, https://doi.org/10.1016/j.wasman.2018.09.012.
[45] S. Tang, C. Zheng, F. Yan, N. Shao, Y. Tang, Z. Zhang, Product characteristics and kinetics of sewage sludge pyrolysis driven by alkaline earth metals, Energy 153 (2018) 921–932, https://doi.org/10.1016/j.energy.2018.04.108.
[46] G. Gasco, M.J. Cueto, A. Méndez, The effect of acid treatment on the pyrolysis behavior of sewage sludges, J. Anal. Appl. Pyrolysis 80 (2007) 496–501, https://doi.org/10.1016/j.jaap.2007.03.009.
[47] E.A. Abdel-Aal, M.M. Rashad, Kinetic study on the leaching of spent nickel oxide catalyst with sulfuric acid, Hydrometallurgy 74 (2004) 189–194, https://doi.org/10.1016/J.HYDROMET.2004.03.005.
[48] P.K. Parhi, K.H. Park, G. Senanayake, A kinetic study on hydrochloric acid leaching of nickel from Ni-Al_2O_3 spent catalyst, J. Ind. Eng. Chem. 19 (2013) 589–594, https://doi.org/10.1016/j.jiec.2012.09.028.
[49] N. Habbache, N. Alane, S. Djerad, L. Tifouti, Leaching of copper oxide with different acid solutions, Chem. Eng. J. 152 (2009) 503–508, https://doi.org/10.1016/J.CEJ.2009.05.020.
[50] N.S. Randhawa, K. Gharami, M. Kumar, Leaching kinetics of spent nickel–cadmium battery in sulphuric acid, Hydrometallurgy 165 (2016) 191–198, https://doi.org/10.1016/J.HYDROMET.2015.09.011.
[51] U.S. EPA, Method 3050B - Acid digestion of sediments, sludges and soils: Revision 2, Washington, DC, 1996.
[52] Z. Wang, L. Xie, K. Liu, J. Wang, H. Zhu, Q. Song, X. Shu, Co-pyrolysis of sewage sludge and cotton stalks, Waste Manag. 89 (2019) 430–438, https://doi.org/10.1016/j.wasman.2019.04.033.
[53] K. Yoo, B.S. Kim, M.S. Kim, J.C. Lee, J. Jeong, Dissolution of magnesium from serpentine mineral in sulfuric acid solution, Mater. Trans. 50 (2009) 1225–1230, https://doi.org/10.2320/matertrans.M2009019.
[54] V. Madakkaruppan, A. Pius, T. Sreenivas, T.S. Sunilkumar, Behaviour of Si, Al, Fe and Mg during oxidative sulfuric acid leaching of low grade uranium ore: a kinetic approach, J. Environ. Chem. Eng. 7 (2019), 103139, https://doi.org/10.1016/J.JECE.2019.103139.
[55] P. Oustadakis, P.E. Tsakiridis, A. Katsiapi, S. Agatzini-Leonardou, Hydrometallurgical process for zinc recovery from electric arc furnace dust (EAFD): Part I: characterization and leaching by diluted sulphuric acid, J. Hazard. Mater. 179 (2010) 1–7, https://doi.org/10.1016/J.JHAZMAT.2010.01.059.
[56] Š. Langová, J. Riplová, S. Vallová, Atmospheric leaching of steel-making wastes and the precipitation of goethite from the ferric sulphate solution, Hydrometallurgy 87 (2007) 157–162, https://doi.org/10.1016/J.HYDROMET.2007.03.002.
[57] S.R.G. Oudenhoven, A.G.J. van der Ham, H. van den Berg, R.J.M. Westerhof, S.R. A. Kersten, Using pyrolytic acid leaching as a pretreatment step in a biomass fast pyrolysis plant: process design and economic evaluation, Biomass Bioenergy 95 (2016) 388–404, https://doi.org/10.1016/J.BIOMBIOE.2016.07.003.
[58] M. Walawalkar, C.K. Nichol, G. Azimi, Process investigation of the acid leaching of rare earth elements from phosphogypsum using HCl, HNO3, and H_2SO_4, Hydrometallurgy 166 (2016) 195–204, https://doi.org/10.1016/J.HYDROMET.2016.06.008.
[59] S.B. Shen, R.D. Tyagi, J.F. Blais, Environ. Technol. Extr. Cr(III) Other Met. Tann. Sludge Miner. Acids, Environ. Technol., 22, 2001, pp. 1007–1014 doi: 10.1080/09593332208618216.
[60] G. Azimi, V.G. Papangelakis, J.E. Dutrizac, Modelling of calcium sulphate solubility in concentrated multi-component sulphate solutions, Fluid Phase Equilib. 260 (2007) 300–315, https://doi.org/10.1016/J.FLUID.2007.07.069.
[61] J. Morillo, J. Usero, I. Gracia, Heavy metal distribution in marine sediments from the southwest coast of Spain, Chemosphere 55 (2004) 431–442, https://doi.org/10.1016/J.CHEMOSPHERE.2003.10.047.
[62] S.M. Safarzadeh, M.S. Bafghi, D. Moradkhani, M. Ojaghi Ilkhchi, A review on hydrometallurgical extraction and recovery of cadmium from various resources, Miner. Eng. 20 (2007) 211–220, https://doi.org/10.1016/J.MINENG.2006.07.001.
[63] M. Li, S. Zheng, B. Liu, H. Du, D.B. Dreisinger, L. Tafaghodi, Y. Zhang, The leaching kinetics of cadmium from hazardous Cu-Cd zinc plant residues, Waste Manag. 65 (2017) 128–138, https://doi.org/10.1016/J.WASMAN.2017.03.039.
[64] E. Rodríguez, M.A. Vicente, A copper-sulfate-based inorganic chemistry laboratory for first-year university students that teaches basic operations and concepts, J. Chem. Educ. 79 (2002) 486, https://doi.org/10.1021/ED079P486.
[65] C.J. Matocha, A.D. Karathanasis, S. Rakshit, K.M. Wagner, Reduction of copper(II) by Iron(II), J. Environ. Qual. 34 (2005) 1539–1546, https://doi.org/10.2134/jeq2005.0002.
[66] P. Halder, S. Kundu, S. Patel, M.H. Marzbali, R. Parthasarathy, K. Shah, Investigation of reaction mechanism and the effects of process parameters on ionic liquid–based delignification of sugarcane straw, Bioenergy Res. 13 (2020) 1144–1158, https://doi.org/10.1007/s12155-020-10134-7.
[67] I.H. Lee, Y.J. Wang, J.M. Chern, Extraction kinetics of heavy metal-containing sludge, J. Hazard. Mater. 123 (2005) 112–119, https://doi.org/10.1016/J.JHAZMAT.2005.03.035.
[68] P. Meshram, B.D. Pandey, T.R. Mankhand, Process optimization and kinetics for leaching of rare earth metals from the spent Ni–metal hydride batteries, Waste Manag. 51 (2016) 196–203, https://doi.org/10.1016/J.WASMAN.2015.12.018.
[69] E. Olanipekun, A kinetic study of the leaching of a Nigerian ilmenite ore by hydrochloric acid, Hydrometallurgy 53 (1999) 1–10, https://doi.org/10.1016/S0304-386X(99)00028-6.
[70] S.A. Channiwala, P.P. Parikh, A unified correlation for estimating HHV of solid, liquid and gaseous fuels, Fuel 81 (2002) 1051–1063, https://doi.org/10.1016/S0016-2361(01)00131-4.
[71] Q. Lu, Z.L. He, P.J. Stoffella, Land application of biosolids in the USA: a review, Appl. Environ. Soil Sci. 2012 (2012) 1–11, https://doi.org/10.1155/2012/201462.
[72] J. Lin, C. Liu, H. Cao, R. Chen, Y. Yang, L. Li, Z. Sun, Environmentally benign process for selective recovery of valuable metals from spent lithium-ion batteries by using conventional sulfation roasting, Green Chem. 21 (2019) 5904–5913, https://doi.org/10.1039/C9GC01350D.
[73] Z. Yang, D. Wang, G. Wang, S. Zhang, Z. Cheng, J. Xian, Y. Pu, T. Li, Y. Jia, Y. Li, W. Zhou, X. Xu, Removal of Pb, Zn, Ni and Cr from industrial sludge by biodegradable washing agents: caboxyethylthiosuccinic acid and itaconic-acrylic acid, J. Environ. Chem. Eng. 9 (2021), 105846, https://doi.org/10.1016/J.JECE.2021.105846.
[74] V. Montenegro, S. Agatzini-Leonardou, P. Oustadakis, P. Tsakiridis, Hydrometallurgical treatment of EAF dust by direct sulphuric acid leaching at atmospheric pressure, 7, Waste Biomass Valorization 2016 (76) (2016) 1531–1548, https://doi.org/10.1007/S12649-016-9543-Z.
[75] G. Mercier, J.F. Blais, F. Hammy, M. Lounès, J.L. Sasseville, A decontamination process to remove metals and stabilise montreal sewage sludge, Sci. World J. 2 (2002) 1121–1126, https://doi.org/10.1100/tsw.2002.201.
[76] J.-F. Blais, N. Meunier, J.-L. Sasseville, R.D. Tyagi, G. Mercier, F. Hammy, Hybrid Chemical and Biological Process for Decontaminating Sludge from Municipal Sewage, B2US, 6, 855, 2005, 256.B2.
[77] H. Strasser, H. Brunner, F. Schinner, Leaching of iron and toxic heavy metals from anaerobically-digested sewage sludge, J. Ind. Microbiol. 14 (1995) 281–287, https://doi.org/10.1007/BF01569940.

[78] D. del Mundo Dacera, S. Babel, Use of citric acid for heavy metals extraction from contaminated sewage sludge for land application, Water Sci. Technol. 54 (2006) 129–135, https://doi.org/10.2166/wst.2006.764.
[79] M.I. Kokkora, D.L. Antille, S.F. Tyrrel, Considerations for recycling of compost and biosolids in agricultural soil, in: A. Dedousis, T. Bartzanas (Eds.), Soil Biol. Soil Eng, 20, Springer, Berlin, Heidelberg, Berlin-Heidelberg, 2010, pp. 195–215, https://doi.org/10.1007/978-3-642-03681-1_13.
[80] Y. Chen, H. Yang, G. Gu, Effect of acid and surfactant treatment on activated sludge dewatering and settling, Water Res. 35 (2001) 2615–2620, https://doi.org/10.1016/S0043-1354(00)00565-0.
[81] J. Liu, Y. Wei, K. Li, J. Tong, Y. Wang, R. Jia, Microwave-acid pretreatment: a potential process for enhancing sludge dewaterability, Water Res. 90 (2016) 225–234, https://doi.org/10.1016/J.WATRES.2015.12.012.
[82] E. Neyens, J. Baeyens, A review of thermal sludge pre-treatment processes to improve dewaterability, J. Hazard. Mater. 98 (2003) 51–67, https://doi.org/10.1016/S0304-3894(02)00320-5.
[83] T.R. Sreekrishnan, R.D. Tyagi, Heavy metal leaching from sewage sludges: a techno-economic evaluation of the process options, Environ. Technol. 15 (1994) 531–543, https://doi.org/10.1080/09593339409385459.
[84] F. Vegliò, R. Quaresima, P. Fornari, S. Ubaldini, Recovery of valuable metals from electronic and galvanic industrial wastes by leaching and electrowinning, Waste Manag. 23 (2003) 245–252, https://doi.org/10.1016/S0956-053X(02)00157-5.
[85] I.H. Lee, Y.C. Kuan, J.M. Chern, Factorial experimental design for recovering heavy metals from sludge with ion-exchange resin, J. Hazard. Mater. 138 (2006) 549–559, https://doi.org/10.1016/J.JHAZMAT.2006.05.090.
[86] M. Sethurajan, P.N.L. Lens, H.A. Horn, L.H.A. Figueiredo, E.D. van Hullebusch, Leaching and Recovery of Metals, in: E.R. Rene (Ed.), Sustainable Heavy Metals Remediation, Springer International Publishing AG, 2017, pp. 161–206, https://doi.org/10.1007/978-3-319-61146-4_6.
[87] V. Gunarathne, A.U. Rajapaksha, M. Vithanage, D.S. Alessi, R. Selvasembian, M. Naushad, S. You, P. Oleszczuk, Y.S. Ok, Hydrometallurgical processes for heavy metals recovery from industrial sludges, Crit. Rev. Environ. Sci. Technol. (2020) 1–42, https://doi.org/10.1080/10643389.2020.1847949.
[88] S. Singh, V. Kumar, D.S. Dhanjal, S. Datta, D. Bhatia, J. Dhiman, J. Samuel, R. Prasad, J. Singh, A sustainable paradigm of sewage sludge biochar: Valorization, opportunities, challenges and future prospects, J. Clean. Prod. 269 (2020), 122259, https://doi.org/10.1016/J.JCLEPRO.2020.122259.
[89] J. Shao, X. Yuan, L. Leng, H. Huang, L. Jiang, H. Wang, X. Chen, G. Zeng, The comparison of the migration and transformation behavior of heavy metals during pyrolysis and liquefaction of municipal sewage sludge, paper mill sludge, and slaughterhouse sludge, Bioresour. Technol. 198 (2015) 16–22, https://doi.org/10.1016/J.BIORTECH.2015.08.147.
[90] International Biochar Initiative, Standardized Product Definition and Product Testing Guidelines for Biochar That Is Used in Soil (aka IBI Biochar Standards), Victor, NY, USA, 2015. ⟨http://www.biochar-international.org/characterizationstandard⟩. (Accessed July 14, 2021).
[91] J.K.M. Chagas, C.C. de Figueiredo, J. da Silva, K. Shah, J. Paz-Ferreiro, Long-term effects of sewage sludge–derived biochar on the accumulation and availability of trace elements in a tropical soil, J. Environ. Qual. 50 (2021) 264–277, https://doi.org/10.1002/jeq2.20183.
[92] A. Méndez, A. Gómez, J. Paz-Ferreiro, G. Gascó, Effects of sewage sludge biochar on plant metal availability after application to a Mediterranean soil, Chemosphere 89 (2012) 1354–1359, https://doi.org/10.1016/j.chemosphere.2012.05.092.